Journal of the Serbian Chemical Society
JSCS@tmf.bg.ac.rs • www.shd.org.rs/JSCS
J. Serb. Chem. Soc. 83 (10) 1143–1156 (2018)
JSCS–5139
UDC 661.34–71+66.046.58–188:551.46:539.4+549.755.122
Original scientific paper

Durability of alkali activated slag in a marine environment: Influence of alkali ion

IRENA NIKOLIĆ[1]*, MILENA TADIĆ[1], IVONA JANKOVIĆ-ČASTVAN[2], VUK V. RADMILOVIĆ[3] and VELIMIR R. RADMILOVIĆ[4]

[1]*University of Montenegro, Faculty of Metallurgy and Technology, Džordža Vašingtona bb, 81 000 Podgorica, Montenegro,* [2]*University of Belgrade, Faculty of Technology and Metallurgy, Karnegijeva 4, 11120 Belgrade, Serbia,* [3]*Innovation Center, Faculty of Technology and Metallurgy, University of Belgrade, Karnegijeva 4, 11120 Belgrade, Serbia and* [4]*Serbian Academy of Sciences and Arts, Knez Mihailova 35, 11000, Belgrade, Serbia*

(Received 28 March, revised 3 July 2018, accepted 4 July 2018)

Abstract: The durability of alkali-activated steel electric arc furnace slag (EAFS) in a marine environment was evaluated with respect to the chemical composition of the alkaline activator. Two different alkaline activators have been used: a mixture of NaOH and Na_2SiO_3 solutions (Na-activator), as well as a mixture of KOH and K_2SiO_3 solutions (K-activator). The obtained results gave the insight into the influence of alkaline activator chemistry on the compressive strength and durability of alkali-activated slag (AAS), which was exposed to the damaging seawater environment. The porosity of AAS was found to be the most important factor with regards to the strength and durability of these materials in marine environment. Sodium based alkali-activated slag (Na-AAS) displayed lower porosity and higher compressive strength compared to potassium based AAS (K--AAS). Lower porosity and thus a lower rate of water uptake by AAS matrix, *i.e.*, the lower sorptivity was exhibited by the Na-AAS when compared to K-AAS. Hence, Na-AAS exhibited better durability in a marine environment.

Keywords: steel slag; seawater; sorptivity; brucite.

INTRODUCTION

The by-products of steel production can generally be classified into three groups: basic oxygen furnace, electric arc furnace and ladle slag. The composition of steel slag is highly variable and primarily depends on the raw material selection and processing conditions. Electric arc furnace slag (EAFS) is mainly comprised of various oxides such as CaO, FeO, Al_2O_3, MgO, MnO, P_2O_5, etc., while the main crystal phases are dicalcium and tricalcium silicates (Ca_2SiO_4 and Ca_3SiO_5, respectively), dicalcium ferrite ($Ca_2Fe_2O_4$) and wüstite (FeO).[1] In Eur-

* Corresponding author. E-mail: irena@ac.me
https://doi.org/10.2298/JSC180328057N

ope, nearly 12 million t of steel slag is produced each year and about 65 % is used in qualified fields of application, while the remaining 35 % ends up on landfills.[2] This slag is primarily used in civil engineering[3–7] but it can have a potential application as a neutralizing agent in bioleaching[8] as well as in aiding phosphorous and heavy metals removal from wastewaters.[9–11]

In the past two decades a lot of attention has been paid to the use of a new class of slag based materials known as alkali-activated slag (AAS). These materials are currently considered as a possible replacement for the ordinary Portland cement (OPC) binder due to its enhanced durability and performance in various environments. The alkali activation process involves a chemical reaction of slag with the alkaline activator which starts with breaking of the Ca–O, Mg–O, Si–O–Si, Al–O–Al and Al–O–Si chemical bonds,[12] followed by the condensation and the hardening processes. Aluminium-containing calcium silicate hydrate gel (C–(A)––S–H) with a low Ca/Si ratio has been identified as a hydration product of slag alkali activation.[13] The structure of C–(A)–S–H gel is similar to the calcium silicate hydrate (C–S–H) structure in OPC, although it is highly amorphous and characterized by a high aluminum content, indicating a high degree of aluminum substitution for silicon in bridging positions.[14] This substitution of Al^{3+} for Si^{4+} generates a charge imbalance, compensated by the uptake of Na^+ or K^+ in the C–(A)–S–H gel.[15] This gel controls the strength development of AAS similarly to C–S–H phase, which is the main hydration product of OPC.

The structure and properties of C–(A)–S–H gel are strongly dependent on the type of alkaline activator present, which greatly affects the properties of AAS.[16] Sodium silicate (Na_2SiO_3)-activated AAS is characterized by higher compressive strength, lower water absorption capabilities, higher workability, higher drying shrinkage and lower porosity in comparison to AAS activated with sodium hydroxide (NaOH).[17,18]

Durability of AAS in aggressive environments is the main advantage of these materials over OPC and thus the behaviour of AAS in a marine environment is of great importance due to the presence of a variety of harmful species. Generally, the cement-based construction elements exposed to an aggressive environment like seawater are at a risk of structural incapability due to the penetration of detrimental elements into the material matrix.[19,20] In this sense, the prevention of protrusion of Cl^- and Mg^{2+} is of great importance. The surface of steel bars incorporated in cement-based building elements is passivated due to the high pH of concrete pore solution. Protrusion of Cl^- ions into the concrete pores leads to the decrease of pH value of pore solution providing the conditions for the corrosion of steel bars. Moreover, the presence of Mg^{2+} in seawater influences the stability of C–S–H gel in cement-based matrix. The exposure of cement based materials to seawater results in leaching of Ca due to the decalcification of the C–S–H gel[19] and to the formation of a non-cementing magnesium silicate

hydrate (M–S–H) by an ion exchange (Mg^{2+} and Ca^{2+}) in the C–S–H.[20] Similar behaviour is proposed for AAS systems in solutions of medium magnesium chloride concentration.[21]

The durability of alkali-activated binders has been widely investigated, but there is little data on the durability of these materials in the marine environment. Previous investigations indicated the high durability of alkali activated slag mortars in seawater from the standpoint of sulphate ions attack.[22] However, the durability issue of AAS is influenced by the chemistry of alkali activator used for the production of AAS mortars. NaOH activated slag mortars exhibit lower porosity than those activated with water glass, which is associated with the structural and compositional differences of the main reaction product. Higher porosity of NaOH activated slag mortars yields higher permeability and higher ingress of sulphate ions, leading to the formation of products of expansive character (gypsum and ettringite) which results in the decrease of the compressive strength.[22]

Moreover, the beneficial use of seawater in the production of AAS was reported.[23] The hardened AAS mixed with seawater has higher strength than the one mixed with tap water, due to the activation of the alkali salts like NaCl, $MgCl_2$, Na_2SO_4 and $MgSO_4$ which accelerate the activation. Besides, the strengthening of AAS mixed with seawater was observed upon further exposure to seawater for a period of up to one year, which is ascribed to the continual activation by seawater, which resulted in forming more reaction product.[23] Although extensive investigations have been carried in the field of AAS, especially in terms of their durability, relatively little is known about the influence of alkaline metal ions on the properties and the durability of AAS in a marine environment. Thus, the aim of this research was to investigate the influence of alkali activator chemistry on the durability of AAS in a marine environment with the AAS synthesized by the alkali activation of EAFS by Na- and K- activators.

EXPERIMENTAL

The EAFS used in this investigation was obtained from the Steel Mill Nikšić in Montenegro and its chemical composition is presented in Table I. Prior to alkali activation EAFS was ground down to a fine powder with a mean particle size of d_{50} = 24 μm, measured on a Malvern 2000 laser particle size analyzer.

TABLE I. Chemical composition of EAFS

Component	CaO	FeO	SiO_2	Fe_2O_3	MgO	MnO	Cr_2O_3	Al_2O_3	TiO_2
Content, %	46.5	23.5	12.2	0.9	6.5	1.3	0.8	7.24	1.06

The AAS samples were synthesized using two types of alkali activators at a constant solid to liquid mass ratio of 4. Na-activator was prepared by mixing 10 M NaOH and commercial liquid Na_2SiO_3 (SiO_2/Na_2O mole ratio of 3.2), while the K-activator was prepared by mixing 10 M KOH and commercial liquid K_2SiO_3 (SiO_2/K_2O mole ratio of 3.2) solutions. The SiO_2/Na_2O mole ratio in Na-activator and SiO_2/K_2O mole ratio in K- activator were 1 and 1.2,

respectively. Accordingly, Na-activator was added as 4.8 and 4.8 mass % of Na_2O and SiO_2, respectively, while K-activator was added as 7.6 and 4.4 mass % of K_2O and SiO_2, respectively.

The paste obtained by the alkali activation was cast in a plastic cylindric mold (28 mm×60 mm), sealed with a lid to prevent the loss of evaporating water and cured for 48 h at 65 °C. Subsequently, the AAS samples were removed from molds and left to rest 14 days in a laboratory room at the temperature of 22±2 °C and 35 % relative humidity before any testing was performed. Durability of Na-AAS and K-AAS was tested by immersing the samples in seawater for a period of 14 weeks. For this purpose, two groups of five AAS samples of the same series (Na- or K-AAS) were exposed to seawater attack. Natural seawater (pH 8.3) was taken for the experiment. Prior to the experiment, seawater was poured into polyethylene flasks and left to stay for a period of 7 days in order to reach the temperature of laboratory room. The volume of seawater was 2 dm^3 per five samples of same series. The volume of each sample was approximately 0.03 dm^3. After this time, the samples were dried and subjected to characterization tests.

Five control AAS samples of each series were tested for compressive strength on an HP--400 hydraulic press at room temperature in aerobic conditions (standard test conditions). Before testing, the surfaces of the sample were polished flat and parallel. The compressive strength measurements were performed according to the MEST EN 1354:2011 standard, using five cylinders of each series and averaging the obtained experimental values.

Both Na-AAS and K-AAS samples were subjected to porosity investigations. Pore size distribution and surface area evaluated using N_2 adsorption/desorption isotherms were obtained using the Micrometrics accelerated surface area and porosity (ASAP) 2020 instrument. To ensure the removal of moisture, degassing of Na-AAS and K-AAS was performed at 100 °C for 24 h.

The qualitative phase analysis of Na-AAS and K-AAS before and after exposure to marine environment as well as EAFS source materials was performed by the X-ray powder diffraction (XRPD) technique on a Philips PW 1710 diffractometer using monochromatized CuKα radiation (λ = 1.54178 Å) and step-scan mode (2θ range from 4 to 90°, step 0.02°, scan speed 0.8 s per step).

Microstructural and chemical investigations were carried out using the FEI Helios NanoLab 660 SEM/FIB dual beam system, equipped with the EDAX energy dispersive spectrometer (EDS). The SEM images were recorded with various electron detectors, including the secondary electron detector (SED).

The capillary water absorption was carried out according to Hall method[24] and can be determined by using the following equation:

$$I = S\sqrt{t} \tag{1}$$

where I is cumulative water absorption per unit area of the inflow surface, S is sorptivity coefficient and t is elapsed time. The sorptivity coefficient (S) can be determined from the slope of the I *vs.* $t^{0.5}$ plot. For this purpose of sorptivity test, the surfaces of AAS samples were exposed to the marine environment. The increase of mass of the samples, measured over regular time periods, was attributed to the water-intake by the capillary pore effect.

RESULTS AND DISCUSSION

Characterization of AAS samples

The results of porosity investigation of Na- and K-AAS samples are summarized in Table II. Although a somewhat larger pore size (pore width) was observed in the case of Na-AAS, the pore volume and specific surface area were significantly lower compared to that of the K-AAS (Table II), which indicate that Na-AAS is less porous in comparison to K-AAS. The results of porosity analysis are in good agreement with the results of strength investigations, as Na-AAS exhibits higher compressive strength, 38.8 MPa than K-AAS, 32.3 MPa (Table II). The similar effect of alkaline activator chemistry on the strength development of the alkali-activated stainless-steel slag was observed in previous research.[25,26] The higher strength of Na-AAS sample in comparison to K-AAS can be attributed to the higher volume of reaction product formed in Na-based alkali activated systems.[25,26] Although the overall activation process is the same, regardless of the type of activator, there is a difference in the dissolution–condensation rates. Due to the difference in charge densities, the smaller Na^+ ions exhibit strong attraction to water and retain their hydration layer of water molecules more efficiently than larger K^+, which do not have strong association with water and readily bind with the negative charge on the silicate.[27,28] Consequently, the hydrated ionic radius of Na^+ is larger than K^+ leading to the better dissolution of starting materials in alkali activator and to the formation of a greater number of oligomers, larger in size, with strong interaction.[28] The increased interactions between dissolved entities lead to the formation of a higher volume of reaction products and better mechanical properties of alkali activated materials. Moreover, it has also been reported that the porosity of alkali activated materials can be varied by the selection of alkali ions, where less porous alkali activated materials are produced when sodium is progressively replaced by potassium.[29]

TABLE II. Cumulative pore volume (V_{cum}), specific surface area (S_{BET}) and compressive strength (σ) of Na-AAS and K-AAS samples; standard deviations are given in parentheses

Sample	S_{BET} / m^2g^{-1}	V_{cum} / cm^3 g^{-1}	Pore width, nm	σ / MPa
Na-AAS	6.5	0.0142	8.7	38.8 (1.6)
K-AAS	17.48	0.0233	5.1	32.3 (1.3)

The XRPD analysis results (Fig. 1) have shown that EAFS, Na-AAS and K-AAS are mostly amorphous materials (broad diffraction hump of 2θ from 28 to 38° centered at approximately 33°). No crystalline C-A-S-H phase was detected by XRPD since the reaction product of slag alkali activation exhibits an amorphous structure in XRPD spectrum. In all samples, the main crystal phases were: wüstite; a complex nonstoichiometric oxide of Fe with the general formula $Fe_{1-x}O$ (JCPDS 89-0686); larnite, β-Ca_2SiO_4 (JCPDS 77-0388); and gehlenite,

$Ca_2Al(AlSiO_7)$ (JCPDS 89-6887). There is a possibility that very small amounts of monticellite, $CaMgSiO_4$ (JCPDS 84-1319), calcite $CaCO_3$ (JCPDS 89-1304), and ilvaite $CaFe_3O(OH)(Si_2O_7)$ (JCPDS 82-1847) were present in all samples as well as δ-Fe (JCPDS 89-4186) in Na-AAS, but due to their small amounts, unambiguous identification based on XRPD measurements was not possible.

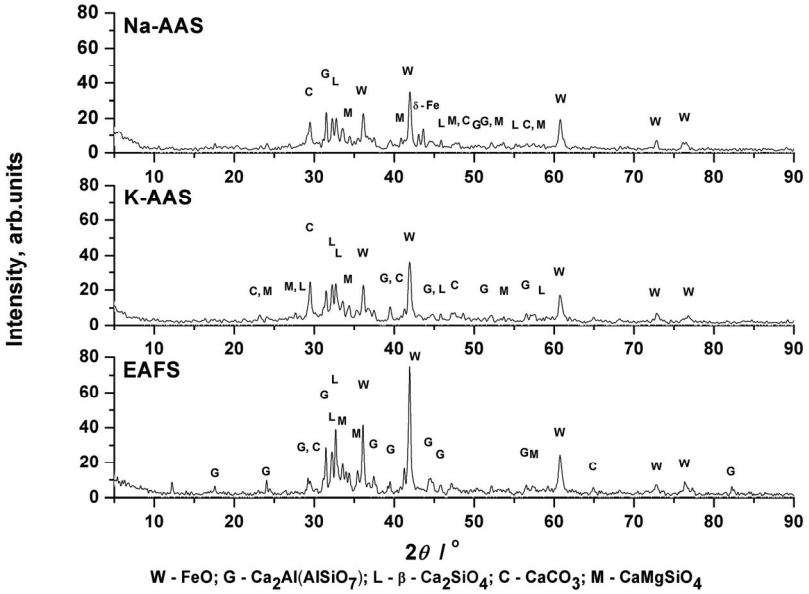

Fig. 1. XRPD patterns of electric arc furnace slag (EAFS) and alkali activated slag (Na-AAS and K-AAS).

The microstructure of Na-AAS and K-AAS is characterized by the presence of unreacted slag bonded by the reaction product of AAS, noted as "A" and "B", respectively, in Fig. 2. The results of EDS analysis of Na-AAS and K-AAS (Table III) indicate the presence of C–(A)–S–H gel, with a high content of alkali

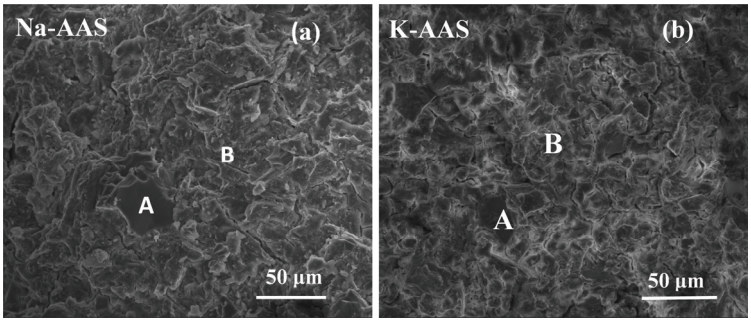

Fig. 2. Microstructure of: a) Na-AAS and b) K-AAS samples; unreacted slag noted as "A" and reaction product of AAS noted as "B".

ions (Na^+ or K^+), as the main reaction product in the alkali activation process. The data in Table III were obtained from the average of 3 sample areas.

TABLE III. The content of main elements and the average Ca/Si content ratio in the reaction product of AAS; standard deviations are given in parentheses

Sample	Content, wt. %					Ca/Si
	Ca	Si	Al	Na	K	
Na-AAS	16.31	17.1	3.62	15.41	–	0.95
	(0.66)	(0.23)	(0.4)	(0.59)		(0.05)
K-AAS	22.25	11.9	4.16	–	6.94	1.87
	(0.79)	(0.36)	(0.12)		(0.41)	(0.01)

The Ca/Si ratios for Na-AAS and K-AAS (B-region) were found to be 0.95 and 1.87, respectively, while the content of the alkaline metals (Na and K) was 15.41 and 6.94 %, respectively. These results are in agreement with the previous results where AAS systems with lower Ca/Si ratios were characterized by higher compressive strength[17] and higher uptake of the alkaline metal ions.[30] The Ca/Si ratio in the reaction product of slag alkali activation is closely related to the conditions of slag dissolution in the alkali activator. Since the choice of alkali ion influences the dissolution of starting materials in the alkali activator, this inevitably leads to the difference in Ca/Si ratio in the reaction product of alkali activation. Our previous investigations[31] indicated a more efficient leaching of silica in the presence of Na^+ than in K^+, which is reflected in the lower Ca/Si ratio in the reaction product of slag alkali activation.

Durability of AAS samples

Durability of Na-AAS and K-AAS exposed to an aggressive seawater environment was evaluated in terms of the mechanical and the microstructural properties, as well as in terms of the crystalline phase formation on the surface of the samples. The strength of Na- and K-AAS samples after seawater attack were 37.8±0.8 MPa and 28.8±1.1 MPa, respectively. It is evident that after immersion in seawater for a period of 14 weeks, both samples displayed certain decrease in strength. The Na-AAS sample exhibited a slight strength loss of 2.5 % while the K-AAS sample exhibited a much higher strength loss of 10.9 %. The results obtained inferred that Na-AAS samples are less sensitive to seawater attack than K-AAS samples. This is in agreement with the findings of Puertas *et al.*[22] who pointed to the porosity of AAS as an important factor in terms of the stability of AAS in seawater. Namely, Na-AAS samples have a lower porosity and thus lower permeability than those made with K-activator. Therefore, Na-AAS samples are more resistant to seawater attack than K-AAS. Immersing Na-AAS and K-AAS in seawater generates an alkaline solution (pH 9.6) due to the ion exchange between the excess Na^+ or K^+ from AAS matrix and H_3O^+ from the

aquatic environment.[32] After a period of 14 weeks, a white layer on the surface of both, Na-AAS and K-AAS, was observed (Fig. 3). The results of the microstructural investigations of the Na-AAS and K-AAS immersed in seawater (Fig. 4) have shown that the corroded layer (A) on the surface of AAS (B) is comprised of mostly Mg and O. This layer acts as a barrier and slows down the penetration of chlorides inside the Na-AAS and K-AAS, thereby protecting them from the aggressive environment.

Fig. 3. Sample of AAS before and after immersion in seawater.

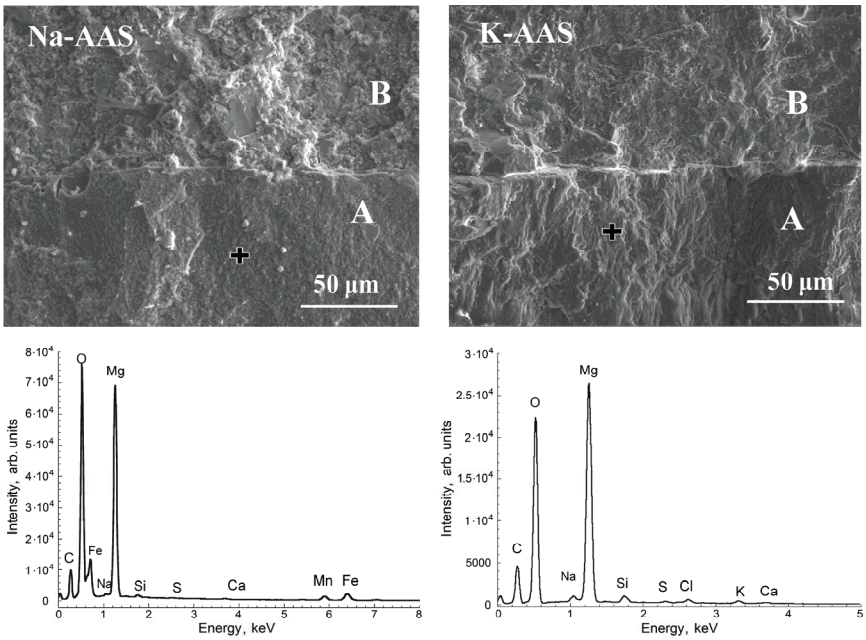

Fig. 4. SEM micrographs and corresponding EDS spectra of Na-AAS and K-AAS after immersion in seawater; corroded layer is noted as "A" and AAS is noted as "B" in micrographs.

Diffraction analysis of these surface corroded layers of Na-AAS and K-AAS revealed the presence of brucite, $Mg(OH)_2$ (about 90 %) and calcite $CaCO_3$ (about 10 %) as the major crystalline phases (Fig. 5) which is in agreement with the findings of SEM/EDS analysis.

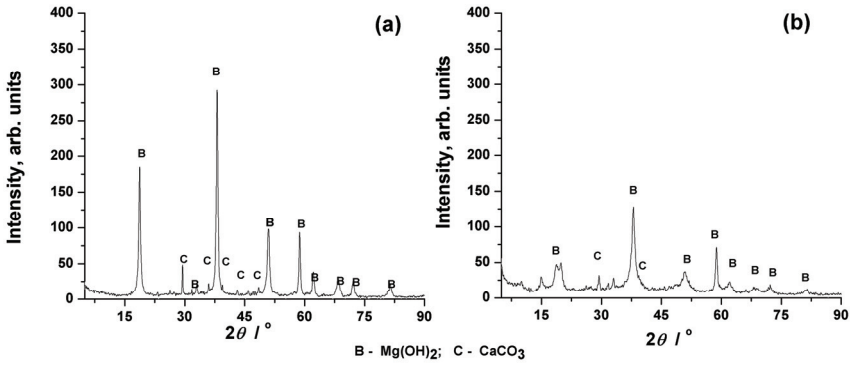

Fig. 5. XRPD patterns of the surface layer on Na-AAS (a) and K-AAS (b) samples after immersion in seawater.

Since the AAS samples in a marine environment generate alkaline solutions, the Mg^{2+} ions from seawater react with the OH^- ions liberated from AAS matrix and precipitate as brucite, $Mg(OH)_2$ (Eq. (2)), as shown by the XRPD and SEM/ /EDS analysis. Additionally, the liberated Ca^{2+} from the AAS matrix in alkaline environment form $Ca(OH)_2$, which reacts with the carbonates from seawater forming calcium carbonate (Eq. (3)) at the surface of the exposed sample, also confirmed by the XRPD analysis:

$$Mg^{2+} + 2OH^- \rightarrow Mg(OH)_2 \quad (2)$$

$$Ca(OH)_2 + H_2CO_3 \rightarrow CaCO_3 + 2H_2O \quad (3)$$

Additionally, EDS line scans have been performed on Na-AAS and K-AAS samples after immersion in seawater, starting from the corroded layer and going into the AAS matrix (Fig. 6).

According to the line scan profiles for both samples, the amount of Mg in the corroded layers (A) is high and rapidly decreases at the interface with the AAS matrix (B). The line scan of both samples indicate the negligible concentrations of Ca, Si and Al in the corroded layers, which rapidly increase at the A/B interface.

The fluctuation of concentration of these elements at the corroded layer/AAS matrix interface is a result of the partial decalcification of the C–(A)–S–H gel when in contact with seawater. From Fig. 6 it is evident that the Na-AAS sample exhibits better resistance to Cl penetration, compared to the K-AAS sample. In both cases, the highest concentration of Cl was observed at the A/B interface, after

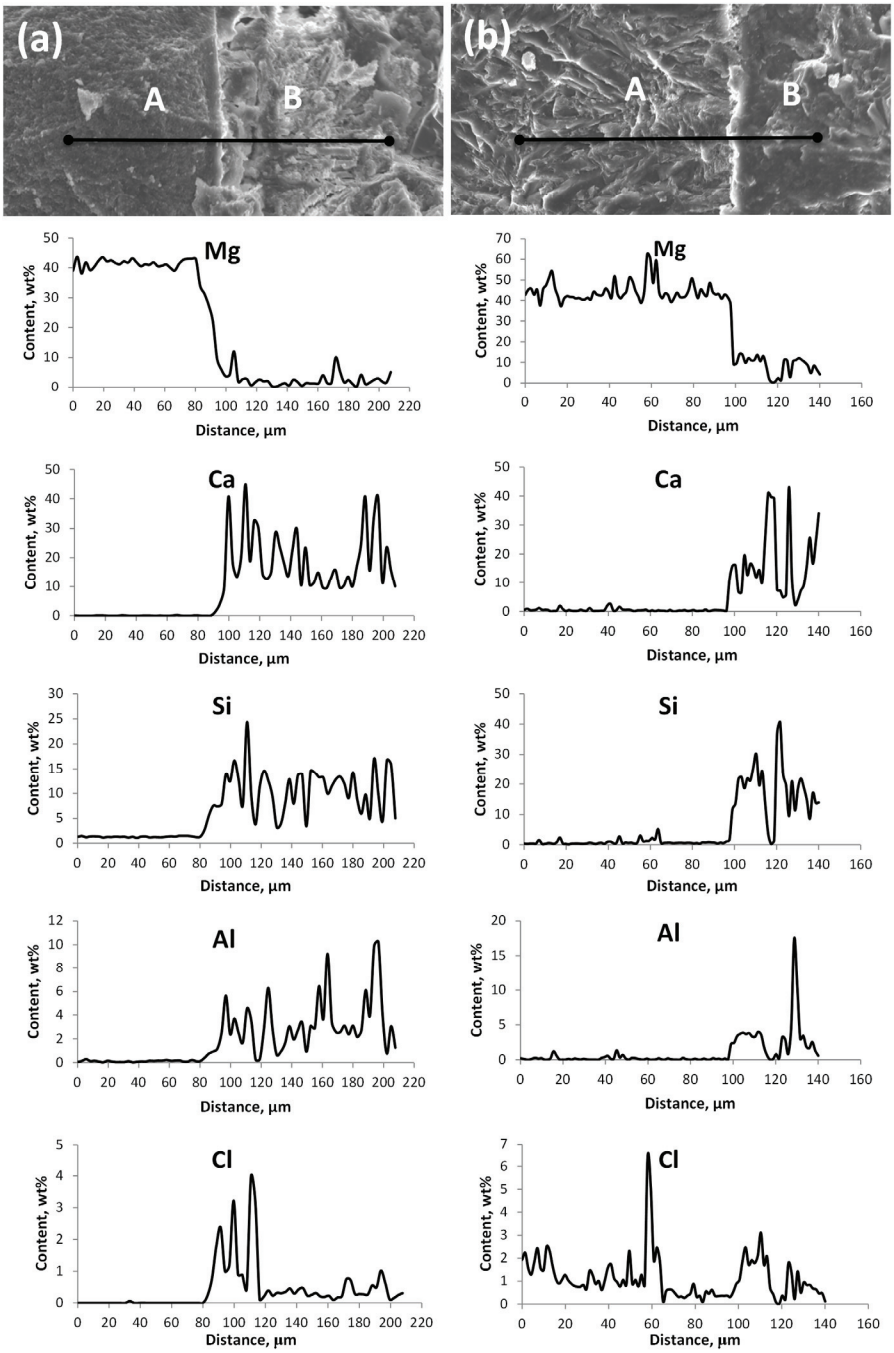

Fig. 6. SEM micrographs noting the direction of EDS line scan profile near corroded layer (A)/AAS matrix (B) interface for (a) Na-AAS and (b) K-AAS, immersed in seawater.

which it decreases going into the AAS matrix. When Na-AAS and K-AAS come in contact with seawater, Cl penetrates into the AAS matrix and remains bonded inside, while the corroded layer was formed on the surface of matrix. The results of EDS line scans indicate that the amount of Cl in the AAS matrix was higher in the case of K-AAS than for the Na-AAS. The main factor which influences the penetration of Cl and other harmful species into the AAS matrix, when in contact with an aggressive environment, is porosity. As shown by the porosity investigations, K-AAS exhibits a higher porosity than Na-AAS, which enables greater diffusion of Cl ions into the K-AAS and thus a higher amount of Cl is observed near the A/B interface of K-AAS. Moreover, the higher amount of Cl ions is also observed in the surface corroded layer formed of K-AAS, than in the surface layer of Na-AAS, which indicates the easier penetration of Cl ions through the corroded layer of K-AAS. This could be attributed to the crystallinity of the corroded layer formed on the surface of the AAS samples, but this assumption requires more detailed research. As shown by the XRPD analysis (Fig. 5), the corroded layer on the surface of the sample K-AAS was less crystalline than the layer formed on the surface of Na-AAS.

Sorptivity of AAS samples

The ingression of Cl from seawater into the AAS matrix is determined by their sorptivity, *i.e.*, by the rate of water uptake by AAS matrix, when exposed to seawater. The sorptivity plots for Na-AAS and K-AAS are given in Fig. 7.

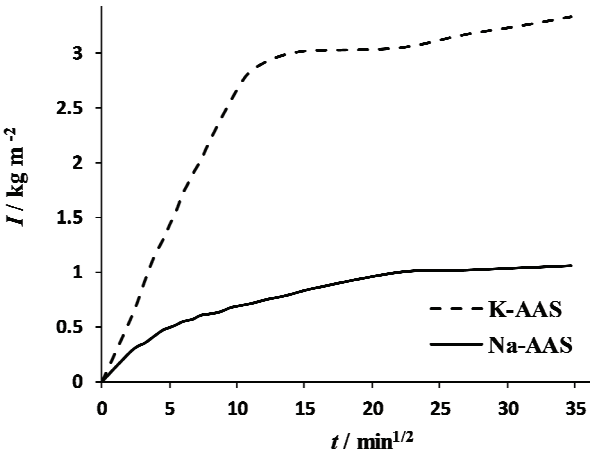

Fig. 7. Cumulative water absorption per unit area of the inflow surface (I) of Na- and K-AAS as a function of the square root of time, *i.e.*, the amount of absorbed water per unit area of the inflow surface.

The calculated values of the capillary sorptivity coefficients (S) are 0.103 and 0.261 kg m^{-2} $s^{-1/2}$ for Na-AAS and K-AAS samples, respectively. The results indicate that the sorptivity of K-AAS is almost double in value than that of Na-AAS. This finding is in agreement with the lower porosity of AAS binder

activated with the Na-activator, which actually controls the ionic transport into the AAS matrix. Higher sorptivity of K-AAS leads to higher Cl uptake and ingression into the K-AAS matrix, as shown by the EDS line scan (Fig. 6).

CONCLUSIONS

The variation of chemical composition of the alkaline activators used for the alkali activation process leads to the significant disparity in terms of the structure of the AAS matrix. A less porous AAS matrix was obtained by using Na-activator, which is associated with higher compressive strength in comparison to the K-AAS, at ambient conditions. The porosity variations, in regards to the type of the alkali ion, also play an important role in the durability of AAS in seawater. The modification of chemistry of the alkaline activator greatly influences the variation in sorptivity of Na-AAS and K-AAS, due, once again, to the difference in the porosity of these samples. Lower sorptivity was observed for the AAS when the Na-activator was used, as the Na-AAS matrix is a less porous structure than K-AAS. Moreover, the formation of a corroded layer, mostly consisting of brucite, $Mg(OH)_2$, on the surface of both Na- and K-AAS samples was observed. It was deduced that this layer has a barrier function which hinders the penetration of Cl^- inside the AAS matrix, and that in turn protects the AAS from the damaging effects of the aggressive marine environment.

ИЗВОД

ПОСТОЈАНОСТ АЛКАЛНО АКТИВИРАНЕ ТРОСКЕ У МОРСКОМ ОКРУЖЕЊУ: УТИЦАЈ АЛКАЛНОГ ЈОНА

ИРЕНА НИКОЛИЋ[1], МИЛЕНА ТАДИЋ[1], ИВОНА ЈАНКОВИЋ-ЧАСТВАН[2], ВУК В. РАДМИЛОВИЋ[3] и ВЕЛИМИР Р. РАДМИЛОВИЋ[4]

[1]Металуршко–технолошки факултет, Универзитет Црне Горе, Цорца Вашингтона бб, 81000 Подгорица, Црна Гора, [2]Технолошко–меалуршки факултет, Универзитет у Београду, Карнегијева 4, 11120 Београд, [3]Иновативни центар, Технолошко–меалуршки факултет, Универзитет у Београду, Карнегијева 4, 11120 Београд и [4]Српска академија наука и уметности, Кнез Михаилова 35, 11000 Београд

Постојаност алкално активиране електропећне челичанске троске у морској води је испитивана у зависности од хемијског састава алкалног активатора. Коришћена су два различита алкална активатора: смеша NaOH и Na_2SiO_3 раствора (Na-активатор) и смеша KOH и K_2SiO_3 раствора (K-активатор). Добијени резултати дају увид у утицај хемијског састава алкалног активатора на притисну чврстоћу и постојаност алкално активиране троске (ААТ) изложене штетном дејству морске воде. Установљено је да је порозност ААТ најзначајнији фактор који утиче на чврстоћу и постојаност ових материјала у морском окружењу. Мању порозност и већу притисну чврстоћу су показали узорци ААТ на бази Na-активатора. Мању порозност, а самим тим мању брзину упијања воде, тј. мању сорпцију, показали су узорци ААТ на бази Na-активатора у поређењу са узорцима на бази K-активатора. Стога, ААТ на бази Na-активатора су показали и бољу постојаност у морском окружењу.

(Примљено 28. марта, ревидирано 3. јула, прихваћено 4. јула 2018)

REFERENCES

1. T. Sofilić, A. Mladenovič, U. Sofilić, *J. Environ. Eng. Landsc. Manage.* **19** (2011) 148 (http://dx.doi.org/10.3846/16486897.2011.580910)
2. H. Motz, J. Geiseler, *Waste Manag.* **21** (2001) 285 (http://dx.doi.org/10.1016/S0956-053X(00)00102-1)
3. S. I. Abu-Eishah, A. S. El-Dieb, M. S. Bedir, *Constr. Build. Mater.* **34** (2012) 2496 (http://dx.doi.org/10.1016/j.conbuildmat.2012.02.012)
4. C. Pellegrino, P. Cavagnis, F. Faleschini, K. Brunelli, *Cem. Concr. Compos.* **37** (2013) 232 (http://dx.doi.org/10.1016/j.cemconcomp.2012.09.001)
5. C. Pellegrino, V. Gaddo, *Cem. Concr. Compos.* **31** (2009) 663 (http://dx.doi.org/10.1016/j.cemconcomp.2009.05.006)
6. S. Wu, Y. Xue, Q. Ye, Y. Chen, *Build. Environ.* **42** (2007) 2580 (http://dx.doi.org/10.1016/j.buildenv.2006.06.008)
7. L. Muhmood, S. Vitta, D. Venkateswaran, *Cem. Concr. Res.* **39** (2009) 102 (http://dx.doi.org/10.1016/j.cemconres.2008.11.002)
8. C. S. Gahan, M. L. Cunha, Å. Sandström, *Hydrometallurgy* **95** (2009) 190 (http://dx.doi.org/10.1016/j.hydromet.2008.05.042)
9. A. Drizo, C. Forget, R. P. Chapuis, Y. Comeau, *Water Res.* **40** (2006) 1547 (http://dx.doi.org/10.1016/j.watres.2006.02.001)
10. N. C. Okochi, D. W. McMartin, *J. Hazard. Mater.* **187** (2011) 250 (http://dx.doi.org/10.1016/j.jhazmat.2011.01.015)
11. L. Ćurković, Š. Cerjan-Stefanović, A. Rastovčan-Mioč, *Water Res.* **35** (2001) 3436 (http://dx.doi.org/10.1016/S0043-1354(01)00037-9)
12. D. Križan, B. Živanović, *Cem. Concr. Res.* **32** (2002) 1181 (http://dx.doi.org/10.1016/S0008-8846(01)00717-7)
13. W. Chen, H. J. H. Brouwers, *J. Mater. Sci.* **42** (2007) 428 (http://dx.doi.org/10.1007/s10853-006-0873-2)
14. A. R. Brough, A. Atkinson, *Cem. Concr. Res.* **32** (2002) 865 (http://dx.doi.org/10.1016/S0008-8846(02)00717-2)
15. P. Duxson, J. L. Provis, *J. Am. Ceram. Soc.* **91** (2008) 386469 (http://dx.doi.org/10.1111/j.1551-2916.2008.02787.x)
16. F. Puertas, M. Palacios, H. Manzano, J. S. Dolado, A. Rico, J. Rodríguez, *J. Eur. Ceram. Soc.* **31** (2011) 2043 (http://dx.doi.org/10.1016/j.jeurceramsoc.2011.04.036)
17. S. Aydin, B. Baradan, *Composites, Part B* **57** (2014) 166 (http://dx.doi.org/10.1016/j.compositesb.2013.10.001)
18. M. Ben Haha, G. Le Saout, F. Winnefeld, B. Lothenbach, *Cem. Concr. Res.* **41** (2011) 301 (http://dx.doi.org/10.1016/j.cemconres.2010.11.016)
19. K. De Weerdt, H. Justnes, *Cem. Concr. Compos.* **55** (2015) 215 (http://dx.doi.org/10.1016/j.cemconcomp.2014.09.006)
20. K. De Weerdt, H. Justnes, M. R. Geiker, *Cem. Concr. Compos.* **47** (2014) 53 (http://dx.doi.org/10.1016/j.cemconcomp.2013.09.015)
21. W. Kurdowski, *Cem. Concr. Res.* **34** (2004) 1555 (http://dx.doi.org/10.1016/j.cemconres.2004.03.023)
22. F. Puertas, R. De Gutiérrez, A. Fernandez-Jimenez, S. Delvasto, J. Maldonado, *Mater. Constr. (Madrid, Spain)* **52** (2002) 55 (http://dx.doi.org/https://doi.org/10.3989/mc.2002.v52.i267.326)
23. H. El-Didamony, A. A. Amer, H. Abd Ela-Ziz, *Ceram. Int.* **38** (2012) 3773 (http://dx.doi.org/10.1016/j.ceramint.2012.01.024)

24. C. Hall, *Mag. Concr. Res.* **41** (1989) 51 (http://dx.doi.org/10.1680/macr.1989.41.147.51)
25. M. Salman, Ö. Cizer, Y. Pontikes, R. Snellings, L. Vandewalle, B. Blanpain, K. Van Balen, *J. Hazard. Mater.* **286** (2015) 211 (http://dx.doi.org/10.1016/j.jhazmat.2014.12.046)
26. A. Dakhane, Z. Peng, R. Marzke, N. Neithalath, *Adv. Civ. Eng. Mater.* **3** (2014) 371 (http://dx.doi.org/https://doi.org/10.1520/ACEM20140005.)
27. J. H. Sharp, E. M. Gartner, D. E. Macphee, *Adv. Cem. Res.* **22** (2010) 195 (http://dx.doi.org/10.1680/adcr.2010.22.4.195)
28. P. Steins, A. Poulesquen, O. Diat, F. Frizon, *Langmuir* **28** (2012) 8502 (http://dx.doi.org/10.1021/la300868v)
29. W. M. Kriven, J. L. Bell, M. Gordon, in *Mechanical Properties and Performance of Engineering Ceramics II Ceramics Engineering Proceedings*, R. Tandon, A. Wereszczak, E. Lara-Curzio (Eds.), John Wiley & Sons, Hoboken, NJ, 2006, pp. 491–498
30. S. Y. Hong, F. P. Glasser, *Cem. Concr. Res.* **32** (2002) 1101 (http://dx.doi.org/10.1016/S0008-8846(02)00753-6)
31. I. Nikolić, A. Drinčić, D. Djurović, L. Karanović, V. V. Radmilović, V. R. Radmilović, *Constr. Build. Mater.* **108** (2016) 1 (http://dx.doi.org/10.1016/j.conbuildmat.2016.01.038)
32. Z. Aly, E. R. Vance, D. S. Perera, J. V Hanna, C. S. Griffith, J. Davis, D. Durce, *J. Nucl. Mater.* **378** (2008) 172 (http://dx.doi.org/10.1016/j.jnucmat.2008.06.015).